# Features of observing for weak MSTIDs by GNSS satellites

R.O. Sherstyukov* [(1)], A.D. Akchurin [(1)], O.N. Sherstyukov [(2)]
(1) Kazan Federal University, Institute of Physics, Kremlevskaya Street 18, Kazan, Tatarstan 420008, Russia

## Abstract

To analyze the weak midlatitude medium-scale travelling ionospheric disturbances we use the sufficiently dense network of GNSS receivers (more than 150 ground-based stations). We show the reason that the monitoring for MSTIDs by GNSS satellites is fragmented. Comparing of satellites R18 and G18 data (at 9:40 UT on September 21, 2016) revealed that the LOS directed to ongoing MSTIDs front is preferred for MSTIDs observing. The characteristics of extremely weak MSTIDs with TECp values ~0.2 TECU, wavelength~ 100 km and western direction of phase front moving are presented. We estimate these characteristics as a threshold for monitoring the MSTIDs by GNSS network we used.

## 1. Introduction

The ionosphere as a whole is fairly quiescent plasma with permanently moving irregularities called travelling ionospheric disturbances (TIDs). Based on scale size, these plasma disturbances divided into three kinds: large, medium and small. At midlatitudes the medium scale traveling ionospheric disturbances (MSTIDs) are dominant. This MSTIDs has been studied for more than 50 years by various instruments: ionosondes [1-4], dense networks of GNSS receivers [5-7], radars of coherent and incoherent scattering [8,9], Doppler radars [10], all sky imagers [11,12], etc.

Midlatitude MSTIDs is usually divided into 3 types: (1) daytime MSTIDs which propagate southeastward and frequently occur in the winter morning and equinoxes; (2) nighttime MSTIDs which propagate southwestward and frequently occur in the summer; (3) dusk MSTIDs which propagate northwestward and frequently occur in summer [6]. Miller et al. suggested that these differences in the MSTIDs characteristics can be due to the different mechanisms of their production [13].

The search for MSTIDs generation mechanisms is complicated by the inconsistency of MSTIDs characteristics (such as dominant propagate direction, intensity of plasma perturbations, phase front speed, wavelength, period) of the data obtained by the researchers. First of all, this is due to the different sensitivity to MSTIDS of different methods of ionosphere diagnostics. Thus, for example, there is no consistency in the appearance of MSTIDs in TEC perturbations and F-spread [14] or U-V-shaped signatures [15]. All research methods have their limitations, therefore, to determine the full spectrum of MSTIDs parameters, it is necessary to designate admissible parameters that a particular method is capable to observe.

The appearance of dense GNSS receiver networks gave the new impetus to observations of ionospheric irregularities. Two-dimensional TEC mapping method allows observing the MSTIDs spatial-temporal dynamics. This method became an important source of information, especially for daytime TIDs, which are not available for all sky imagers.
In this study we show the problems of TEC-mapping method while working near the sensitivity threshold and the results of observing for weak midlatitude MSTIDs.

## 2. Method and Results

In our investigation more than 150 GPS/GLONASS receiving points were used. Figure 1 shows the location of GPS/GLONASS receivers. All GPS/GLONASS receivers provide the data of carrier phase and pseudo-range measurements in two frequencies (f1 = 1575.42 MHz, f2 = 1227.60 MHz for GPS receivers and f1=1602+n×0.5625 MHz , f2= 1246 MHz +n×0.4375 MHz for GLONASS receivers, there n is the number of frequency channel (n =−7,−6,−5,…0,…,6). The GPS/GLONASS data are converted to two-dimensional TEC perturbation maps for TID investigation.
The TEC perturbation component derived by detrending slant TEC with one-hour running average for each line-of-sight (see [16] for more details). The TEC perturbation value for each pixel of TEC map is an average of perturbations for all lines-of-sight which crossed the pixel at 250 km altitude (the approximate F-region peak height). The size of each pixel is 0.15×0.15 in latitude and longitude. TEC map in each epoch is smoothed spatially with the running average of 5×5 pixel (0.75×0.75) in latitude and longitude.

The daytime MSTIDs are enough weak at midlatitudes, it means that their wavelength could be less than 100 km, and intensity of perturbation could be less than 10%. Such characteristics of MSTIDs make them practically invisible for TEC mapping technique.
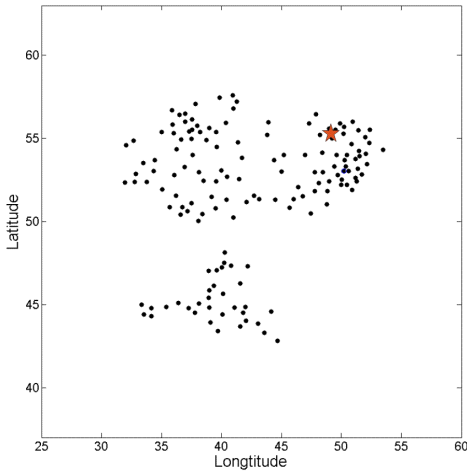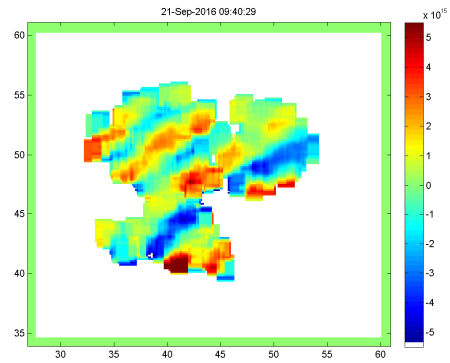
**Figure 1**. Location of GNSS receivers

There are a number of reasons: (i) The perturbed TEC magnitude of observed TIDs significantly depends on the angle between TID phase front and satellite-receiver line-of-sight (see [17] for more details). The best condition for TIDs detecting is the parallelism of the phase front of TID and satellite-receiver line-of-sight. (ii) The distance between the cells of the receiver network imposes a restriction on the minimum observing wavelength of the TIDs by TEC-mapping technique.

Using the TEC data we make two-dimensional TEC perturbation maps for 2 satellites observing the MSTIDs with various angle of line-of-sight (LOS) for the same time. Figures 2,3 shows two-dimensional TEC perturbation maps over European part of Russia in the daytime at 09:30 UT on September 21, 2016, using the data of GPS (G18) and GLONASS (R18). It may be noted that for G18 the band structure (signature of the MSTIDs) with wavelength ~200 km and perturbed TEC (TECp) magnitude ~0.4 TECU on two-dimensional TEC perturbation maps can be observed, but R18 at the same time is blind.

We consider the position of LOS for both satellites relative to the phase front of MSTIDs at 09:40 - 10:30 UT. In Figure 4 the direction of MSTIDs phase front moving and the direction of ionospheric pierce points moving (for G18 and R18 satellites) are shown. It is seen that at 9:40, the LOS of R18 satellite directed towards the outgoing phase front of MSTIDs. The G18 satellite occupies an almost opposite position but shifted along the azimuth from the direction of MSTIDs phase front moving.

According to the data of incoherent scattering radar [18], the phase fronts of MSTIDs are inclined from the vertical. Therefore, the LOS directed to ongoing MSTIDs front is preferred for MSTIDs observing, because as was noted the TEC perturbed magnitude grows when the phase front of TID and satellite-receiver LOS are in parallel. If the satellite radio signal passes through the whole thickness
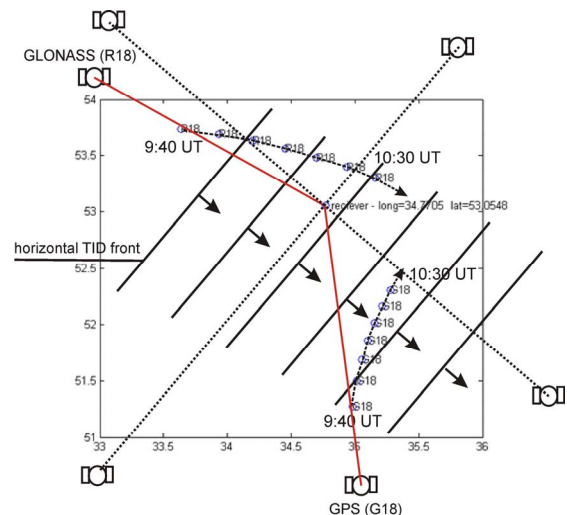
of enhancement/depletion band, the TECp magnitude might be high, but if the satellite radio signal passes enhancement and depletion band, the TECp magnitude tends to zero values.



**Figure 2**. TEC-map plotted using the R18 data at 9:30 UT on September 21, 2016
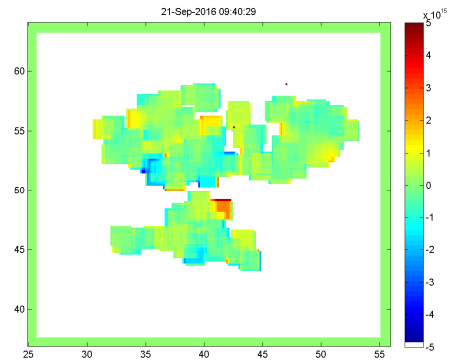


**Figure 3**. TEC-map plotted using the R18 data at 9:30 UT on September 21, 2016



**Figure 4**. Location of GNSS receiver, satellites (G18, R18) and MSTIDs band structure. Red lines indicate the receiver-satellite LOS, black lines indicate phase fronts of MSTIDs, black arrows show the direction of phase front moving

In shematic figure 5 the LOS with good conditions for MSTIDs detection are marked by blue lines, the LOS with bad conditions for MSTIDs detection are marked by red lines. This figure clearly shows the problems of satellite monitoring of plasma perturbations such as MSTIDs.
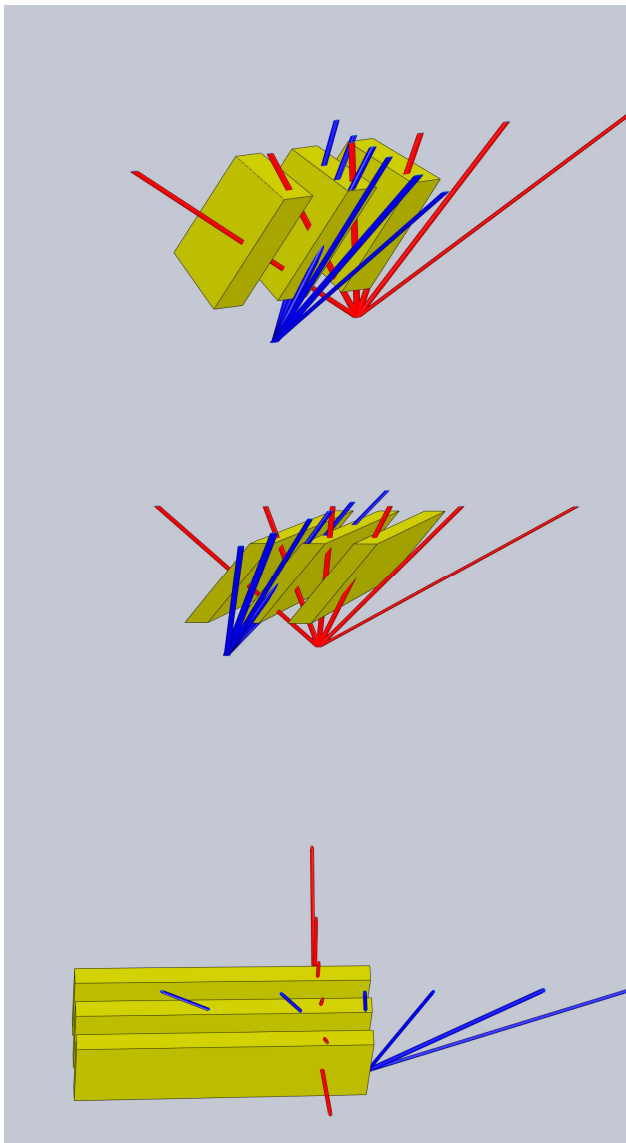


**Figure 5**. Shematic image of inclined MSTIDs and satellite-recieverLOS. The LOS with good conditions for MSTIDs detection are marked by blue lines, the LOS with bad conditions for MSTIDs detection are marked by red lines.

We estimate that for our GNSS network the weakest MSTIDs that are available for detecting could have wavelength >80 km, and TECp > 0.2 TECU. To detect the parameters of such weak MSTIDs is a great rarity, because the detection conditions (parallelism of LOS and phase front) must be excellent. In figure 6 the band structures of weak MSTIDs at 15:30 UT on September 22, 2016 with TECp~0.2 TECU, wavelength ~100 km, and western direction of phase front moving are shown. We suppose that these MSTIDs have intensity of perturbation dN/N less than 10%, because they are not seen in foF2 variations by ionosonde data.
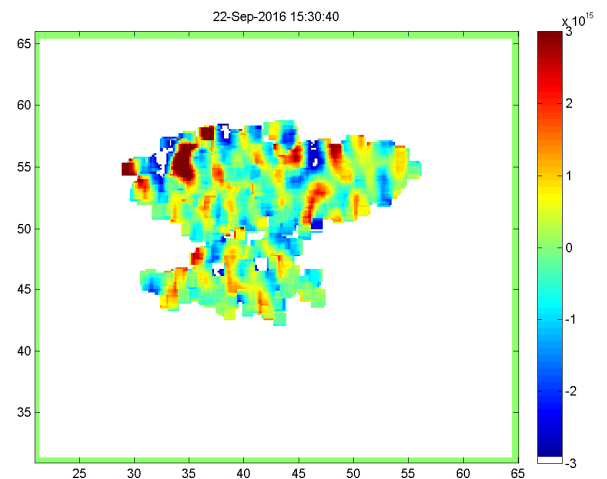


**Figure 6**. TEC-map plotted using the R18 data at 9:30 UT on September 21, 2016

## 3. Discussions and Conclusions

In this study the problems of transionospheric sounding by GNSS satellites are shown. Some weak MSTIDs remain undetected, because the detection conditions depend on the angle between satellite-receiver LOS and MSTIDs phase front. So the monitoring of MSTIDs by GNSS satellites is fragmented. The correct statistic of parameters can be obtained only for sufficiently large MSTIDs, with intensity of perturbations dN/N>30%, and wavelength >250 km. We assume that this is the reason for the differences in the intensity of the appearance of MSTIDs by the data of GNSS and ionosonde. It is necessary to reliably understand the sensitivity thresholds of both methods to MSTIDs, in order to correctly compare the data. Comparing of satellites R18 and G18 data (at 9:40 UT on September 21, 2016) shows that the LOS directed to ongoing MSTIDs front is preferred for MSTIDs observing. It means that MSTIDs are inclined from the vertical and it is coincides with observations of other researches.

The two-dimensional TEC perturbation map with weak MSTIDs are presented. We estimate the characteristics of MSTIDs as: the magnitude of TECp ~0.2 TECU, the wavelength~ 100 km. The direction of phase front moving does not match to dominant. Therefore, we believe that taking into account the characteristics of weak MSTIDs is an important for formation of reliable theory of MSTIDs generation.

## 6. Acknowledgements

# 7. References

1.      Booker H., The role of acoustic gravity waves in the generation of spread-F and ionospheric scintillation, Journal of Atmospheric and Terrestrial Physics, Vol. 41, No. , P. 501-515, 1979.

2.      Booker, H. G., P. K. Pasricha, and W. J. Powers, Use of scintillation theory to explain frequency-spread on F-region ionograms, J. Atmos. Terr. Phys., 48, 327354, 1986.

3.      Bowman, G. G., Movements of ionospheric irregularities and gravity waves, J. Atmos. Terr. Phys., 30, 721-734, 1968.

4.      Bowman, G. G.,  A review of some recent work on mid-latitude spread-F occurrence as detected by ionosondes, J. Geomag. Geoelectr., 42, 109-138, 1990.

5.      Saito, A., Miyazaki, S., and Fukao, S.: High resolution mapping of TEC perturbations with the GSI GPS network over Japan, Geophys. Res. Lett., 25, 3079–3082, 1998.

6.      Kotake, N., Otsuka, Y., Tsugawa, T., Ogawa, T., and Saito, A.: Statistical study of medium-scale traveling ionospheric disturbances observed with the GPS networks in Southern California, Earth Planets Space, 59, 95–102, 2007.

7.      Otsuka, Y., Kotake, N., Shiokawa, K., Ogawa, T., Tsugawa, T., and Saito, A.: Statistical Study of Medium-Scale Traveling Ionospheric Disturbances Observed with a GPS Receiver Network in Japan, Aeronomy of the Earth's Atmosphere and Ionosphere, IAGA Special Sopron Book Series, Vol. 2, Part 3, 291–299, doi:10.1007/978-94-007-0326-1 21, 2011.

8.      Ogawa, T., N. Nishitani, Y. Otsuka, K. Shiokawa, T. Tsugawa, and K. Hosokawa (2009), Medium-scale traveling ionospheric disturbances observed with the SuperDARN Hokkaido radar, all-sky imager, and GPS network and their relation to concurrent sporadic E irregularities, J. Geophys. Res., 114, A03316.

9.      Djuth, F. T., Zhang L. D., Livneh D. J., Seker I., Smith S. M., Sulzer M. P., Mathews J. D., and Walterscheid R. L. (2010), Arecibo's thermospheric gravity waves and the case for an ocean source, J. Geophys. Res., 115, A08305, doi:10.1029/2009JA014799.

10.     Georges, T. M. (1968), HF Doppler studies of traveling ionospheric disturbances, J. Atmos. Terr. Phys. 30, 735-746.

11.     Seker, I., D. J. Livneh, and J. D. Mathews (2009), A 3-D empirical model of F region Medium-Scale Traveling Ionospheric Disturbance bands using incoherent scatter radar and all-sky imaging at Arecibo, J. Geophys. Res., 114, A06302, doi:10.1029/2008JA014019.

12.     Lee, C. C., Y. A. Liou, Y. Otsuka, F. D. Chu, T. K. Yeh, K. Hoshinoo, and K. Matunaga (2008), Nighttime medium-scale traveling ionospheric disturbances detected by network GPS receivers in Taiwan, J. Geophys. Res., 113, A12316, doi:10.1029/2008JA013250.

13.     Miller, C. A., W. E. Swartz, M. C. Kelley, M. Mendillo, D. Nottingham, J. Scali, and B. Reinisch, Electrodynamics of midlatitude spread F, 1. Observations of unstable, gravity wave-induced ionospheric electric fields at tropical latitudes, J. Geophys. Res., 102, 11,521–11,532, 1997.

14.     Kotake, N., Otsuka, Y., Tsugawa, T., Ogawa, T., and Saito, A.: Climatological study of GPS total electron content variations caused by medium-scale traveling ionospheric disturbances, J. Geophys. Res., 111, A04306, 2006, doi:10.1029/2005JA011418.

15.     Sherstyukov, R.O., Akchurin A.D., Sherstyukov O.N., Collocated ionosonde and dense GPS/GLONASS network measurements of midlatitude MSTIDs. Advances in Space Reseach, 2017, https://doi.org/10.1016/j.asr.2017.11.026.

16.     Tsugawa, T., Otsuka, Y., Coster, A.J., Saito, A., Medium-scale traveling ionospheric disturbances detectedwith dense and wide TEC maps over North America. Geophys. Res. Lett. 34, L22101, 2007.

17.     Afraimovich, E.L., Terekhov, A.I., Udodov, M.Iu., Fridman, S.V., Refraction distortions of transionospheric radio signals caused by changes in a regular ionosphere and by travelling ionospheric disturbances. J. Atmos. Terr. Phys. 54, 1013–1020., 1992

18.     Djuth, F. T., L. D. Zhang, D. J. Livneh, I. Seker, S. M. Smith, M. P. Sulzer, J. D. Mathews, and R. L. Walterscheid, Arecibo's thermospheric gravity waves and the case for an ocean source, J. Geophys. Res., 115, A08305, 2010, doi:10.1029/2009JA014799.